AN EXPRESSION FOR THE NEAR-FACE DISPLACEMENT OF D-SHAPED TUNNELS UNDER ANISOTROPIC IN SITU STRESS CONDITIONS

Miguel A. Nunes, Graduate Student, McGill University, Montréal, Québec, Canada
Mohamed A. Meguid, Assistant Professor, McGill University, Montréal, Québec, Canada

ABSTRACT
This paper seeks to conduct an investigation into the effects of elastic bi-directional in-situ stress distributions in isotropic media in terms of radial closure along the entire length of the cavity, with specific attention given to the near-face region. The results presented are obtained from a parametric study based on full three-dimensional finite element analyses. The data are benchmarked using existing field data from the Darlington Intake Tunnel in Southern Ontario. The results of the study are then used for developing a simple expression and charts for predicting wall displacements along the entire length of a tunnel subjected to different in-situ stress conditions.

RÉSUMÉ
Cet article cherche à conduire une recherche sur les effets des distributions bi-directionnelles élastiques d'effort in-situ dans des médias isotropes en termes de fermeture radiale sur la longueur entière de la cavité; une attention spécifique étant donnée à la région proche de la face. Les résultats présentés sont obtenus à partir d'une étude paramétrique basée sur une analyse tridimensionnelle complète à l'élément fini. La validation des données fut accompli en utilisant des données de champ obtenues du tunnel de prise de Darlington en Ontario méridional. Les résultats de l'étude sont alors employés pour développer une expression simple et des diagrammes pour prévoir les déplacements de mur sur la longueur entière d'un tunnel soumis à de différentes conditions d'effort in-situ.

NOMENCLATURE

a: Variable Tunnel Radius (m)
d: Distance from Tunnel Face (m)
γ: Unit Weight (kN/m^3)
E: Young's Modulus (GPa)
K_0: Coefficient of Lateral Earth Pressure
$m_1, m_2, m_3, n_1, n_2, n_3$: Empirical Constants
ν: Poisson's Ratio
Ω: Normalised Displacement (dimensionless)
P_0: Average Principal Stress (GPa)
R: Constant Tunnel Radius (m)
u: Radial Tunnel Displacement (μm, mm)

1. INTRODUCTION

Some civil engineering projects such as hydroelectric works, transportation networks, and electricity power plants make use of tunnels for their operation, which can enhance the efficiency of these projects. However, the construction of structures that are located at the surface do not have the added challenges associated with subterranean conditions, or more specifically, those that arise from in-situ stresses due to overlaying soil or rock.

It is therefore of interest to the engineer to gain a comprehensive understanding of how these forces will affect the displacements around the opening of a tunnel as it is excavated, and how they are enhanced or altered by working under differing in-situ stress conditions. The observed displacements around the periphery of the tunnel are the result of the re-distribution of in-situ stresses. The first tool at the engineer's disposal is elasticity theory which can be applied to provide an initial estimation of these circumferential displacements about a tunnel opening. Although the behaviour of soil or rock material is never truly elastic (nor the properties ever isotropic), the simplicity of all elastic solutions that predict stresses and displacements present an adequate preliminary insight into the effect of various parameters. To this end, much work exists in the literature that seeks to describe, model and predict these parameters, most notably of which are circumferential displacements.

2. NUMERICAL MODELLING

This paper is concerned primarily with the longitudinal displacements that occur after a tunnel has been excavated in elastic and isotropic media, especially in the region immediately preceding the face advance, typically about four to five tunnel radii away from the face. The prototype that was used for the numerical model was that of the Darlington G.S. in Pickering, Ontario. The geometry of this tunnel is presented in Figure 1 as a half-space. The calculated displacement data were benchmarked against measured field data acquired via extensometers. A more detailed discussion is presented in the example in Section 5.

The analyses were performed using the Plaxis 3D-Tunnel finite element program employing 15-noded wedge elements. The 3D finite element analysis was performed using 7020 fifteen-noded isoparametric wedge elements with a total of 19991 nodes arranged as shown in Figure 2. Nodes along the vertical boundaries of the mesh may translate freely along the boundaries but are fixed against displacements normal to these boundaries. The nodes at the base are fixed against displacements in both directions. The stage of excavation which is depicted in the figure is the final phase.

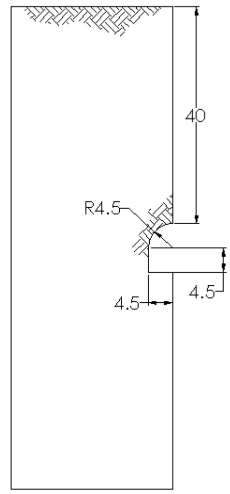

Figure 1: Geometry of the Darlington G.S. Tunnel

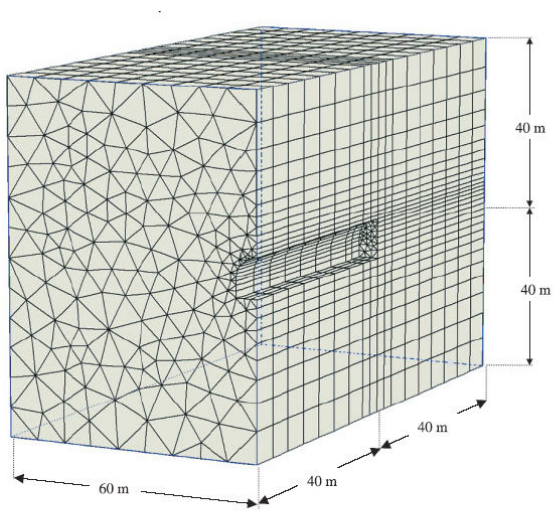

Figure 2: 3-D Mesh based on the Darlington G.S. Tunnel (Meguid and Rowe, 2006)

3. METHODOLOGY

Three variables, E, ν and γ were used in a parametric study. E varied from 20 to 30 GPa, ν from 0.27 to 0.33, γ from 20 to 25 kN/m^3, and each of these cases was analysed for K_0 = 1, 2, 4, 6, 8, 10. To check the numerical results of this analysis against existing solutions, the cases for K_0 = 1 were plotted against the solutions provided by Panet and Guenot (1982) and by Corbetta et al. (1991). A typical example of the tunnel convergence is shown in Figure 3, and it can be seen that the calculated displacements matched quite favourably with the predicted values of the solutions mentioned above.

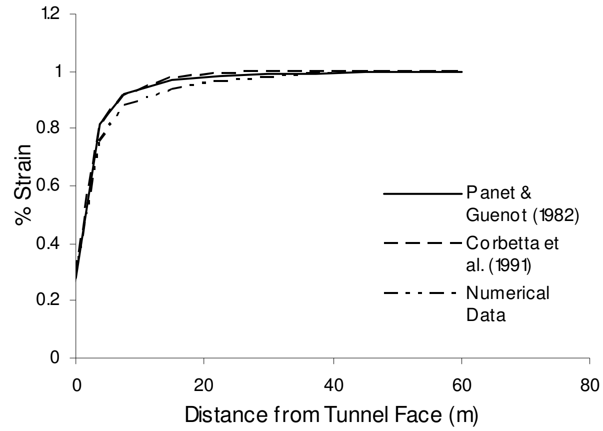

Figure 3: Graphical Comparison of Numerical Predictions with Existing Solutions.

The plane-strain data at the springline and crown in the numerical model were also compared with the analytical solutions provided by Hefny & Lo (1999). The values at the crown matched quite well, whereas the values at the springline were always within at least 86% of the predicted value. This difference can be explained by the fact that the analytical solution was based on an ideal circular opening in an elastic medium, while the numerical model that was used was based on a D-shaped tunnel. Each set of data was trimmed to show only the displacements beginning at the face of the tunnel wall, and ending where apparent plane-strain conditions existed. Displacements were then normalised according to the relation

$$\Omega = \frac{uE}{aP_0}$$

and plotted versus distance from the tunnel face (Ω vs. *d*). Regression was performed, and equations describing the predicted displacements were produced for the crown and for the springline.

4. RESULTS

Certain trends were noticed after examining all of the data. They can be seen in the following figures. It should be noted that all figures in the sections hereafter depict the typical trends mentioned above and were gleaned from the parametric study. Vertical dashed lines indicate the location of the tunnel face, and negative values denote inward or expanding wall movements.

4.1 Effect of Varying Elastic Parameters

At 20 GPa (ν = 0.33, γ = 25 kN/m^3) the plane-strain displacement at the crown was estimated at 0.62 mm, and at 4.3 mm at the springline; while at 30 GPa, the values were 0.41 mm and 2.9 mm respectively. This was a direct consequence of the strength of the medium increasing. Changing ν also had a significant effect, as a value of ν = 0.30 (E = 30 GPa, γ = 25 kN/m^3) had displacements of 0.59 mm and 3.2 mm for crown and springline, respectively. When the value was changed to $\nu = 0.27$, the displacements were 0.64 mm and 2.90 mm, respectively. The variation of the unit weight had the least effect on the displacements. For $\gamma = 20$ kN/m^3 ($\nu = 0.33$, E = 30 GPa) the displacements were 0.33 mm and 2.3 mm, and for $\gamma = 22.5$ kN/m^3 they were 0.37 mm and 2.6 mm.

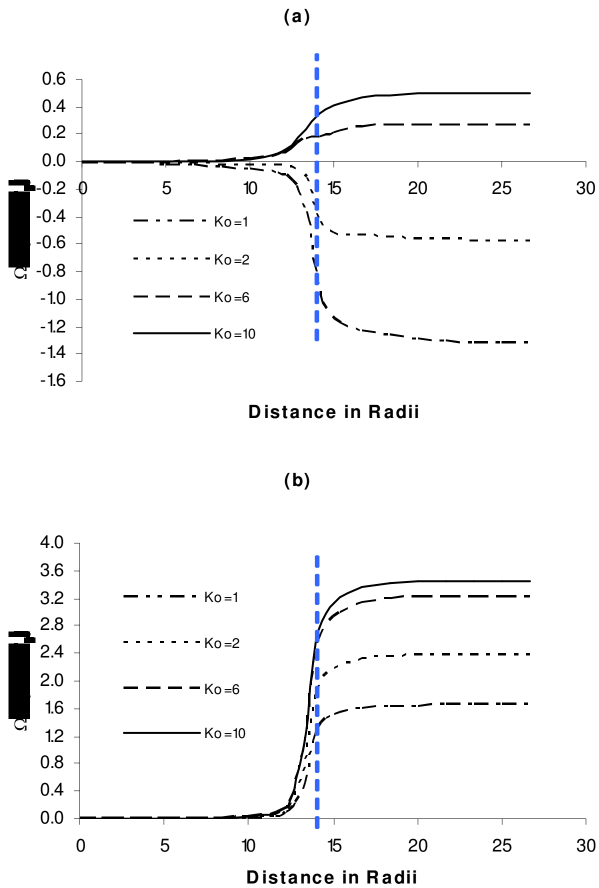

Figure 4: Typical Normalised Displacement Profiles at the (a) Crown, and (b) Springline.

4.2 Displacement at the Tunnel Face

It can also be of interest to investigate the movement of the face of an opening in soft ground or soft rock (Figure 5). Typical displacement patterns are presented in Figures 6, 7 and 8. Negative displacements denote inward or concave movements, whereas positive values represent outward, bulging or convex behaviour.

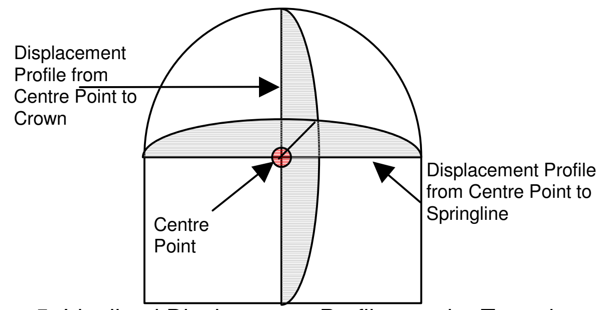

Figure 5: Idealised Displacement Profiles on the Tunnel Face.

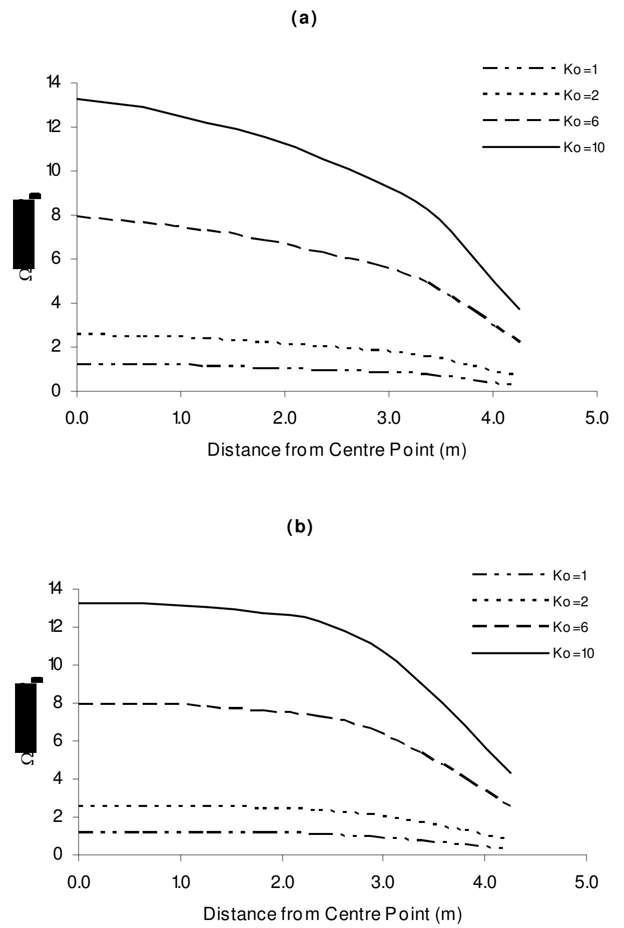

Figure 6: Typical Normalised Displacement Profiles at the face from the centre point to the (a) Crown, and (b) to the Springline. ($\gamma = 20$ kN/m^3, E = 20 GPa, $\nu = 0.27$)

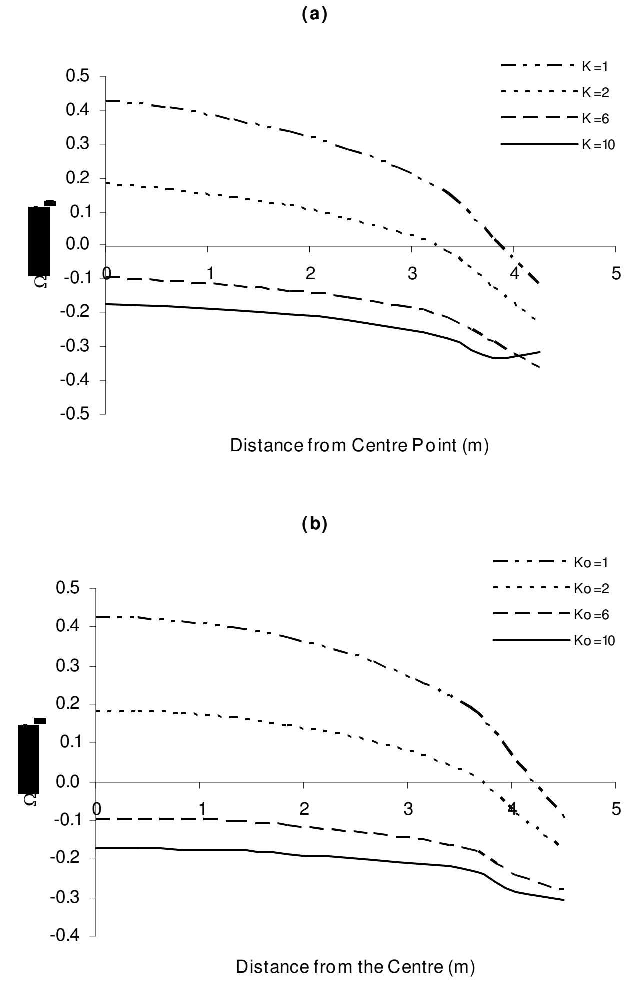

Figure 7: Typical Normalised Displacement Profiles at the face from the centre point to the (a) Crown, and (b) to the Springline. (γ = 22.5 kN/m^3, E = 25 GPa, ν = 0.30)

5. PREDICTING DISPLACEMENTS

The Darlington G.S. case allowed for significant benchmarking of the data. Insodoing it also facilitated the generation of two parametric equations that were used to estimate the displacements at the crown and springline on the tunnel periphery for any given value of E, γ, ν, or K_0. The equations are empirical and take the forms as follows:

$$u_c = \frac{0.259 m_1 R P_0}{E}\left[1.926 m_2 - \exp\left(\frac{-0.605 m_3 d}{R}\right)\right]$$

$$u_s = \frac{2.363 n_1 R P_0}{E}\left[1.455 n_2 - \exp\left(\frac{-1.354 n_3 d}{R}\right)\right]$$

where u_c represents the displacements at the crown, and u_s represents the displacements at the springline. m_1, m_2, m_3 and n_1, n_2, n_3 are constants that are dependent on E, γ, ν, and K_0. The equations were created by performing regression on normalised displacement values for each

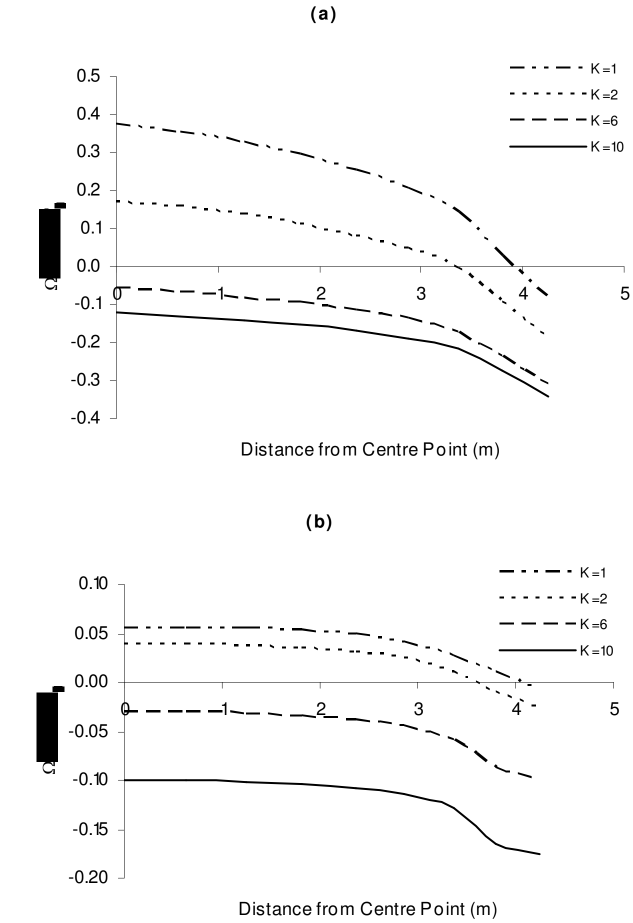

Figure 8: Typical Normalised Displacement Profiles at the face from the centre point to the (a) Crown, and (b) to the Springline. (γ = 25 kN/m^3, E = 30 GPa, ν = 0.33)

trial. The data were truncated where the face of the tunnel was modelled and extended until the tunnel opening. Therefore these equations are valid from the face of the tunnel (d = 0) until a relatively large distance away from the face ($d = \infty$).

6. EXAMPLE: THE DARLINGTON TUNNEL

The Darlington G.S. is a D-shaped nuclear electricity generating facility situated 60 km east of Toronto. The overburden at the site varies between 21 to 36 m consisting of surficial lacustrine deposits and varved silt and clay which is underlain by dense to very dense sandy to silty tills. Beneath the overburden, the first 8 m of rock is a dark brown fossiliferous thin to medium bedded shaly limestone of Whitby Formation. The next 50 m of rock is limestone of the Lindsey Formation, which is mainly a fine-grained, fossiliferous, and massively bedded grey limestone. Testing on rock samples from the site showed that E_h = 46 GPa. The ratio between the horizontal to vertical modulus (E_h:E_v) varied from 1.1 to 1.5, at an average of 1.2. Therefore the rock was weakly anisotropic (Lo and Lukajic, 1984). Please refer to Figures 9 and 10 for detailed views of the Darlington site.

Extensometer	Chainage	Absolute Displacement (Field Data, mm)	Equivalent Chainage	Displacement (Numerical, mm)
A	0+34.6	0.74	0+37.5	0.56
B		0.30		0.40
C		0.20		0.22
D	0+36	2.3	0+37.5	2.1
E		1.8		1.2
F		0.5		0.3

Table 1: Comparison of Field Data with Numerical Data

High horizontal stresses are common in the rock formations in Southern Ontario; it was found that the ratio of the horizontal to vertical initial stresses is approximately 10 at the springline (Lo and Lukajic, 1984).

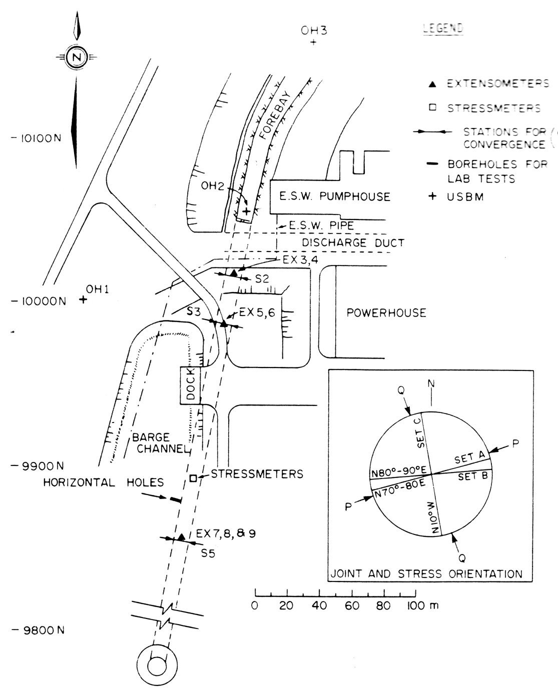

Figure 9: Plan View of the Darlington G.S. (Lo and Lukajic, 1984)

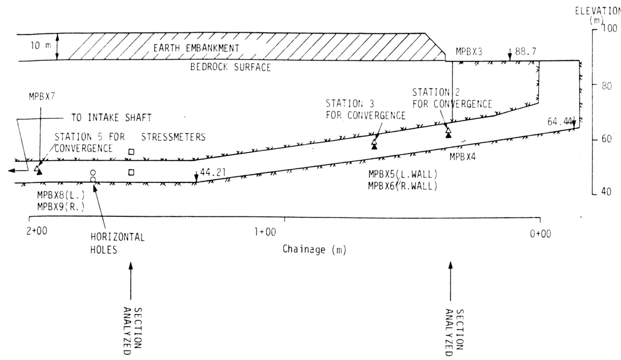

Figure 10: Elevation View of the Darlington G.S. (Lo and Lukajic, 1984)

The field data were then used to validate the numerical model for this case, and a comparison is presented in Table 1. These site data were recovered from extensometers that were placed during the excavation process of the Darlington Tunnel. The constants generated by the regression procedure were then tabulated and were normalised relative to the Darlington example. The observed field displacements and the numerically predicted displacements compared relatively well. A direct comparison was not possible, as the nodes in the mesh did not correspond exactly with the physical location of the extensometers; the closest nodes were chosen instead. As can be seen in Table 1 the values were of the same order, and the authors felt this level of compatibility was sufficient.

7. CONCLUSION

A preliminary description of the displacement profile near the advancing face of the tunnel under differing lateral stress conditions for isotropic elastic media was presented. The parametric study that followed facilitated a simple tool for predicting the longitudinal displacement profile near the face as well as for the plane-strain regions. It was based on full, three-dimensional finite-element analyses. The results were checked against field measurements taken at the Darlington Tunnel of Southern Ontario. While an elastic solution is not realistic, it provides the engineer with a means for acquiring an excellent initial prediction of the longitudinal displacement profile in a tunnel as described above.

8. ACKNOWLEDGEMENTS

This research is supported by the « Fonds Québécois de la recherche sur la nature et les technologies» (FQRNT) and a McGill University Research Grant

REFERENCES

Abdel-Meguid, M, Rowe, R.K and Lo, K.Y. 2003. Three-dimensional analysis of unlined tunnels in rock subjected to high horizontal stress. Canadian Geotechnical Journal, 40(6), 1208-1224.

Carter, J.P., Booker J.R. (1990): Sudden Excavation of a Long Circular Tunnel in Elastic Ground. *Int. J. Rock Mech. Min. Sci. & Geomech.* 27, 129 – 132.

Corbetta, F., Bernaud, D., Nguyen-Mihn, D. (1991): Contribution à la Méthode Convergence-Confinement par le Pricinpe de la Similitude. *Rev. Franç. Géotech*. 54, 5 – 11.

Eringen, A.C. (1957): Elasto-Dynamic Problem Concerning the Spherical Cavity. *Q. J. Mech. Appl. Math*. 10, 257 – 270.

Hefny, A.M., Lo, K.Y. (1999): Analytical Solutions for Stresses and Displacements Around Tunnels Driven in Cross-Anistropic Rocks. *International Journal for Numerical and Analytical Methods in Geomechanics*. 23, 161 – 177.

Kumar, Prabhat (1986): Stress Concentration Due to Underground Excavation in Cross-Anisotropic and Nonhomogeneous Elastic Halfspace. *Computers & Structures*. 25, 687 – 694.

Lo, K.Y., Lukajic, B. (1984): Predicted and Measured Stresses and Displacements Around the Darlington Intake Tunnel. *Can. Geotech. J*. 21, 147 – 165.

Meguid, M.A., Rowe, R.K. (2006): Stability of D-shaped tunnels in a Mohr–Coulomb material under anisotropic stress conditions. *Can. Geotech. J*. 43, 273 – 281.

Morgan, H.D. (1961): A Contribution to the Analysis of Stress in a Circular Tunnel. *Géotechnique*. 11, 37 – 46.

Muir Wood, A.M. (1975): The Circular Tunnel in Elastic Ground. *Géotechnique*. 25, 115 – 127.

Panet, M., Guenot, A. (1982): Analysis of Convergence Behind the Face of a Tunnel. In: Tunnelling '82. The Institution of Mining and Metallurgy, London, 197 – 204.

Pender, M.J. (1980): Elastic Solutions for a Deep Circular Tunnel. *Géotechnique*. 30, 216 – 222.

Selberg, H.L. (1952): Transient Compression Waves from Spherical and Cylindrical Cavities. *Ark. Fys*. 5, 97 – 108.

Sharan, S.K. (1989): Finite-Element Analysis of Underground Openings. *Int. J. Num. & Ana. Meth. Geomech*. 13, 565 – 570.

Sharpe, J. A. (1941): The Production of Elastic Waves by Explosion Pressures. *Geophys*. 7, 144 – 154.

Singh, B., Goel, R.K., Mehrotra, V.K., Garg, S.K., Allu, M.R. (1998): Effect of Intermediate Principal Stress on Strength of Anisotropic Rock Mass. *Tunnelling and Underground Space Technology*. 13, 71 – 79.

Singh, M., Singh, B., Choudhari, J.B., Goel, R.K. (2004): Constitutive Equations for 3-D Anisotropy in Jointed Rocks and Its Effect on Tunnel Closure. *Int. J. Rock Mech. Min. Sci*. 41, 1 – 6.

Tonon, F., Amadei, B. (2002): Effect of Elastic Anisotropy on Tunnel Wall Displacements Behind a Tunnel Face. *Rock Mech. Rock Engng*. 35, 141 – 160.

Verruijt, A. (1997): A Complex Variable Solution for a Deforming Circular Tunnel in an Elastic Half-Plane. *International Journal for Numerical and Analytical Methods in Geomechanics*. 21, 77 – 89.

Xiao, B., Carter, J.P. (1993): Boundary Element Analysis of Anisotropic Rock Masses. *Engineering Analysis with Boundary Elements*. 11, 293 – 303.